Supporting Information

Dynamics of Protein and Peptide Hydration

by Kristofer Modig, Edvards Liepinsh, Gottfried Otting and Bertil Halle

Pulse Sequences Used for NOE Experiments on Oxytocin

NOE-NOESY and ROE-NOESY spectra were acquired with pulse sequences described previously,[S1] except that the water magnetization was excited by a train of six 7.5 ms Gaussian 90° pulses, the first five of which were followed by a non-selective 90° pulse of opposite phase and a 1 ms field-gradient pulse to saturate peptide magnetization and avoid radiation damping and demagnetization effects (Fig. S1).[S2] Furthermore, the water resonance was suppressed by a jump-return sequence at the end of the second mixing time τ_{m2}, bipolar gradients (0.25 G m^{-1}) were applied during the evolution time t_1,[S3] a 45° phase-shifted 90° pulse was inserted after t_1,[S4] and a long (200 ms) τ_{m2} value was used to allow for recovery of the water magnetization by radiation damping. With these modifications, the schemes provided effective water flip-back. For improved water suppression, a 1.5 ms gradient pulse (3.75 G cm^{-1}) was applied immediately before the jump-return sequence. To avoid echo effects, gradient pulses were applied during the selective water excitation sequence with 40, 20, 10, 5 and 2.5 G cm^{-1}, respectively. To avoid radiation damping, gradient pulses (1 ms, 3.75 G cm^{-1} and 28 ms, 0.5 G cm^{-1}) were also used during the first mixing time τ_{m1} of the NOE-NOESY experiment. Other experimental parameters were: t_{1max} = 28.5 ms, t_{2max} = 146 ms, τ_{m1} = 30 ms (NOE-NOESY) or 15 ms (ROE-NOESY), jump-return delay τ_{JR} = 0.1 ms, and ROE spin-lock amplitude 15.4 kHz. The total duration of each experiment was 11 h. A control experiment with τ_{m1} = 4 μs (and no gradient pulses during τ_{m1}) produced no diagonal peaks. The nonuniform excitation profile of the jump-return sequence was corrected after Fourier transformation by multiplication of the data by $1/\sin(\Omega\,\tau_{JR})$, where Ω is the offset from the carrier frequency.

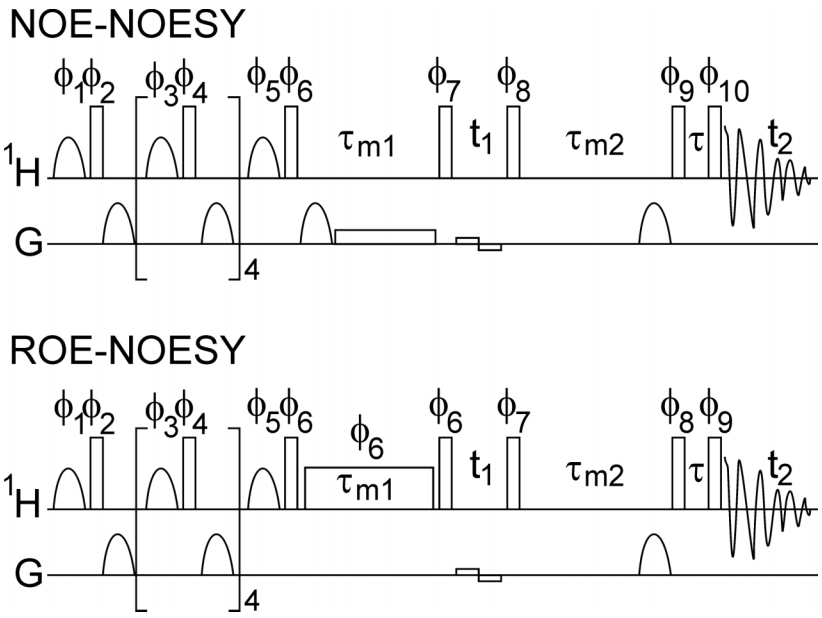

Figure S1. NOE-NOESY and ROE-NOESY pulse sequences. The phase cycle of the NOE-NOESY sequence was: $\phi_1 = 64(x), 64(-x)$; $\phi_2 = -\phi_1$; $\phi_3 = 32(x), 32(-x)$; $\phi_4 = -\phi_3$; $\phi_5 = x, -x$; $\phi_6 = 2(x), 2(-x)$; $\phi_7 = 4(x), 4(-x)$; $\phi_8 = 16(45°), 16(135°)$; $\phi_9 = 8(x), 8(-x)$; $\phi_{10} = -\phi_9$; rec = $(x,-x,-x,x), 2(-x,x,x,-x), (x,-x,-x,x), (-x,x,x,-x), 2(x,-x,-x,x), (-x,x,x,-x)$. The phase cycle of the ROE-NOESY sequence was: $\phi_1 = 32(x), 32(-x)$; $\phi_2 = -\phi_1$; $\phi_3 = 16(x), 16(-x)$; $\phi_4 = -\phi_3$; $\phi_5 = x, -x$; $\phi_6 = 2(y), 2(-y)$; $\phi_7 = 8(45°), 8(135°)$; $\phi_8 = 4(x), 4(-x)$; $\phi_9 = -\phi_8$; rec = $x,-x, x,-x,-x,x,-x,x$.

Compared to conventional NOESY and ROESY experiments without selective water excitation, the NOE-NOESY and ROE-NOESY experiments offer several important advantages: (*i*) arbitrarily short mixing times τ_{m1} can be used without interference from the water suppression scheme that follows τ_{m2}; (*ii*) a water flip-back effect is readily achieved by radiation damping during the long mixing time τ_{m2} together with a jump-return sequence before signal detection; (*iii*) broad exchange cross-peaks are virtually absent from the diagonal, since they relax strongly during τ_{m2};[S5] (*iv*) in case of overlapping diagonal peaks, cross-peaks can be evaluated for quantitative comparison of water-peptide NOEs obtained by NOE versus ROE mixing.

Parameter Values Used for Interpretation of NOE Data on Oxytocin Hydration

To interpret the NOE data on oxytocin hydration in terms of the nonuniform diffusion model, we need to specify values for several parameters. The solvent-accessible radius, b, of oxytocin was set to 10 Å. This value was obtained by adding the minimum distance of closest approach, d_{min} = 2.5 Å, between a water proton and an oxytocin proton (essentially the van der Waals diameter of hydrogen) to the 7.5 Å maximum of the peak in the radial distribution function for the observed NOE protons (relative to the geometric center of oxytocin in the crystal structure 1XY1[S6]). For each oxytocin proton, the distance of closest approach to water protons was calculated as $d = b - \rho$, where ρ is the radial coordinate of the oxytocin proton in the crystal structure. In cases where this produced an unphysically small (< 2.5 Å) d value, we used $d = d_{min}$. The resulting d values are included in Table 4. The water proton number density was set to $n_H = 2\times0.70/0.030 = 47$ nm^{-3}, taking into account that the solvent contains 30 vol% acetone and using 30 Å^3 for the volume occupied by one water molecule. Because both σ_L and σ_R are proportional to n_H, their ratio is independent of n_H. The thickness δ of the hydration layer (with reduced water mobility) and the relative dynamic perturbation D_{bulk}/D_{hyd}, were assigned values consistent with the MRD results. On the assumption that $D_{bulk}/D_{hyd} \approx \langle\tau_\alpha\rangle/\tau_{bulk}$ in a given sample, we took $D_{bulk}/D_{hyd} = 3$ (slightly higher than the MRD value to account for the lower acetone concentration in the cryosolvent used for the NOE experiments). Because $\langle\tau_\alpha\rangle$ refers to $N_\alpha = 73$ water molecules in contact with oxytocin, consistency requires that $N_\alpha V_W = 4\pi[(b + \delta)^3 - b^3]/3$, where V_W is the volume occupied by one water molecule (30 Å^3). With b = 10 Å, we thus obtain δ = 1.5 Å.

From α-carbon ^{13}C relaxation rates, the rotational correlation time, τ_R, of oxytocin has previously been determined to 2 ns at 6 °C in a 90%H_2O/10%D_2O mixture.[S7] To scale this τ_R value to our conditions, we need the viscosity of the cryosolvent at –25 °C. The viscosity of a 90%H_2O/10%D_2O mixture at –25 °C is 6.5 cP.[S8] At +25 °C, addition of acetone to H_2O at a mole fraction acetone of 0.095 (as in our cryosolvent) increases the viscosity by 46%.[S9] Viscosity data at higher acetone mole fractions indicate that the viscosity enhancement factor decreases only slightly as the temperature is lowered from +10 to –10 °C.[S10] Accordingly, we

estimate the viscosity of our cryosolvent at –25 °C as $\eta_0 = 1.4 \times 6.5 = 9.1$ cP. Scaling the experimental τ_R value in proportion to η_0/T (and using $\eta_0 = 1.52$ cP for 90%H_2O/10%D_2O at 6 °C), we thus arrive at $\tau_R = 13.5$ ns in our cryosolvent at –25 °C.

For the oxytocin samples investigated by MRD at –25 °C, we obtain in the same way τ_R = 13 ns (50% H_2O/50% D_2O) and 19 ns (cryosolvent).

The translational diffusion coefficient, D_{bulk}, of bulk water at –25 °C is 3.56×10^{-10} m^2 s^{-1} in H_2O and 2.32×10^{-10} m^2 s^{-1} in D_2O.[S11] Because η_0 varies linearly with the mole fraction D_2O,[S12] we expect that $1/D_{bulk}$ also varies linearly. We then obtain D_{bulk}(10% D_2O) = 3.38×10^{-10} m^2 s^{-1}. This value is reduced further by the presence of acetone. If we assume that $1/D_{bulk}$ and $R_{bulk}(^{17}O)$ have the same linear dependence on the acetone mole fraction, we find that D_{bulk}(10% D_2O) should be reduced by a factor 1/1.4. The same factor is obtained if $1/D_{bulk}$ is scaled by the viscosity of the cryosolvent (see above). Accordingly, our estimate for the translational diffusion coefficient of water at –25 °C in the bulk cryosolvent used for the NOE experiments is $D_{bulk} = 2.4 \times 10^{-10}$ m^2 s^{-1}. The diffusion coefficient that enters the model is actually the sum of the water and oxytocin diffusion coefficients, but, because of the large difference in molecular size, the oxytocin contribution can be neglected.

Parameter Values Used for Interpretation of NOE Data on BPTI Hydration

For the interpretation of NOE data on BPTI hydration in terms of the nonuniform diffusion model, we used the following parameter values. The solvent-accessible radius of BPTI was set to $b = 15$ Å. This value was obtained by adding the minimum distance of closest approach, $d_{min} = 2.5$ Å, between a water proton and a BPTI proton, to the 12.5 Å peak separation in the radial distribution function for the observed NOE protons (relative to the geometric center of BPTI) in the crystal structure 5PTI1.[S13] All the examined BPTI protons are highly exposed and we therefore set $d = d_{min}$ for all of them. As for oxytocin, we make the identification $D_{bulk}/D_{hyd} = \langle \tau_\alpha \rangle / \tau_{bulk}$, but with $D_{bulk}/D_{hyd} = 2$. For consistency, the thickness δ of the hydration layer in the nonuniform diffusion model was determined by the requirement

that the perturbed layer contains N_α = 268 water molecules. This gave δ = 2.4 Å. The water proton number density was set to n_H = 2/0.030 = 67 nm^{-3} and for the bulk water diffusion coefficient we used D_{bulk} = 1.2×10^{-9} m^2 s^{-1}.[S11] The rotational correlation time of BPTI was taken to be τ_R = 6.7 ns, viscosity and temperature scaled from the value determined by ^{15}N relaxation at a BPTI concentration of 3 mM.[S14] At the high BPTI concentration used for the NOE study, as much as 20% of the protein may be present as decamers,[S15] with 8-fold longer τ_R.[S15] BPTI self-association could produce (negative) intermolecular BPTI-BPTI NOE contributions and alter the solvent-accessibility of some surface protons, but these potential complications were neglected in our analysis.

In these calculations, contributions to σ_L and σ_R from intramolecular NOEs to hydroxyl and carboxyl protons, which exchange rapidly with water at pH 3.5, were included. A pK_a value of 4.0 was used for all carboxyl groups. Exchange-relayed NOEs to amino and guanidinum protons were neglected at the low pH used in the NOE study. Contributions from the long-lived internal water molecules in BPTI were also included. For both labile protons and internal water molecules, we used the intramolecular spectral density in eq 8, with the interproton separation r_{HH} computed from the crystal structure 5PTI.[S13]

For the analysis of the MRD data, the rotational correlation time of BPTI at –10 and –30 °C in water of our isotope composition was estimated as follows. From the known viscosities of H_2O and D_2O at these temperatures,[S8] an assumed linear dependence of the water viscosity η_0 on the ^{2}H fraction (as demonstrated at higher temperatures[S12]), and a small (1.8%) oxygen isotope correction, we obtain η_0 = 3.29 cP at –10 °C and 14.75 cP at –30 °C. A ^{15}N relaxation study of 3 mM BPTI (10% ^{2}H, pH* 4.7) at 25 °C yielded τ_R = 3.5 ns.[S14] Assuming that τ_R is proportional to η_0/T, as predicted by hydrodynamics, we obtain τ_R = 14 ns at –10 °C and 70 ns at –30 °C.

Effects of Intermediate Water Exchange Rates on MRD Data for BPTI

In the interpretation of the MRD data for BPTI, one must allow for the possibility that some of the internal water molecules exchange with bulk water at a rate that is not much higher than the local spin relaxation rate in the hydration site. When this is the case, the parameters of the β dispersion must be regarded as apparent parameters, related to the true (fast-exchange) parameters in eqs 5 and 6 by

$$\frac{\tau_{\beta,\mathrm{app}}}{\tau_\beta} = \frac{(N_\beta S_\beta^2)_{\mathrm{app}}}{N_\beta S_\beta^2} = [1 + \omega_\mathrm{Q}^2 S_\beta^2 \tau_\beta \tau_\mathrm{W}]^{-1/2} \qquad \text{(S1)}$$

Figure S2 shows how the apparent quantities vary with the water residence time τ_W under the conditions of the present study.

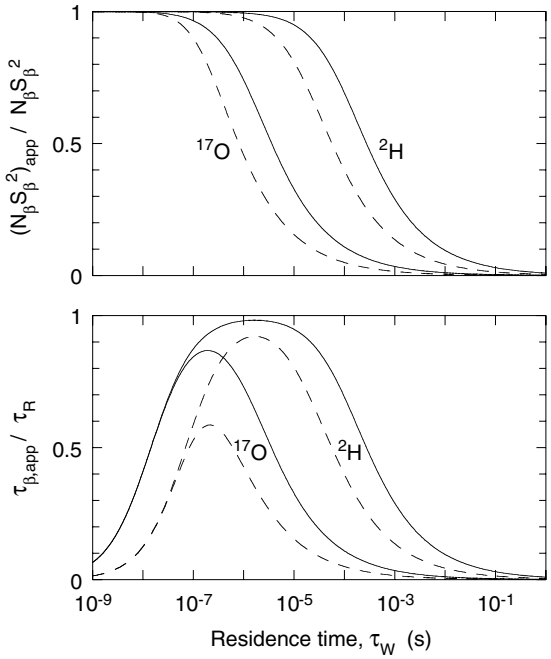

Figure S2. Apparent water ^{2}H and ^{17}O amplitude parameters (upper panel) and correlation times (lower panel) versus the water residence time τ_W. The solid and dashed curves refer to a rotational correlation time τ_R of 14 and 70 ns, respectively, as appropriate for the investigated BPTI solution at –10 and –30 °C. The curves were calculated from eqs 6 and S1, with $S_\beta = 1$.

A comparison with previously reported ^{2}H MRD data for BPTI at similar pH but higher temperatures[S16–S18] is complicated by the presence of a significant decamer fraction at the higher BPTI concentrations used in those studies.[S15] Reanalyzing ^{2}H MRD data[S16] from BPTI at pH* 5.2 and 27 °C taking into account an estimated[S15] 32% decamer fraction, we obtain $(N_\beta S_\beta^2)_{app} = 2.4 \pm 0.2$ and $N_\alpha \left(\langle \tau_\alpha \rangle / \tau_{bulk} - 1 \right) = 950 \pm 50$. The singly buried internal water molecule W122, with a residence time of 170 μs at 27 °C,[S16] contributes 0.7 to $(N_\beta S_\beta^2)_{app}$. The remaining 1.7 units must be due to two or all three of the remainign internal water molecules (W111 – W113). At –10 °C, W122 exchanges too slowly ($\tau_W \approx 50$ ms) to contribute and this is probably the case also for the most deeply buried W113. The dispersion observed at –10 °C is then due to W111 and W112.

According to Fig. S2, the ^{2}H dispersion at –10 °C can be accounted for by one water molecule (W111) with $\tau_W \approx 30$ ns and $\tau_{\beta,app} = 9.7$ ns, contributing 1.0 unit to $(N_\beta S_\beta^2)_{app}$, and another (W112) with $\tau_W \approx 50$ μs and $\tau_{\beta,app} = 11.6$ ns, contributing 0.8 units to $(N_\beta S_\beta^2)_{app}$. This interpretation is supported by the ^{17}O MRD data at –10 °C (Fig. 4b), yielding parameters that differ slightly, but significantly, from the corresponding ^{2}H values (Table 5). According to Fig. S2, essentially the entire ^{17}O dispersion can be accounted for by W111, with $(N_\beta S_\beta^2)_{app} = 0.99$ and $\tau_{\beta,app} = 9.7$ ns, while W112 yields $(N_\beta S_\beta^2)_{app} = 0.2$ and $\tau_{\beta,app} = 2$ ns, causing $N_\alpha \left(\langle \tau_\alpha \rangle / \tau_{bulk} - 1 \right)$ to be larger than for ^{2}H.

At –30 °C, residence times on the order of 1 s are expected for W113 and W122, which therefore do not contribute at all to the ^{2}H dispersion. Also the contribution from W112, with an estimated residence time in the ms range, should be negligibly small. For W111, we expect a residence time in the range 0.1 – 1 μs. It should then contribute fully ($N_\beta S_\beta^2 \approx 1$) with a correlation time close to $\tau_R = 70$ ns (Table 1). However, this scenario is inconsistent with the data, which indicate that the residence time of W111 is either shorter than at –10 °C (unlikely) or very much longer (ms range). The latter might be the case if a local structural transformation takes place between –10 and –30 °C, which reduces the solvent exposure of this water molecule.

Analysis of NOE Data for BPTI

Table S1 compares experimental σ_L/σ_R ratios for BPTI with the corresponding ratios calculated with the aid of the nonuniform diffusion model and parameter values from Table 2. Figure S3 presents results of model calculations with the same parameter values.

Table S1. Experimental and calculated NOE Results for BPTI at 4 °C

		σ_L/σ_R	
Residue	Proton [a]	Exp't	Theory [b]
Leu-6	δ^2H (3)	0.5–1.0	0.29
Lys-15	αH (1)	0.5	0.17
Lys-15	δH (2)	0.7	0.33
Lys-15	εH (2)	0.5	0.34
Arg-17	δH (2)	0.3	0.43
Ile-18	αH (1)	0.2	0.36
Ile-18	γH (2)	0.5–1.0	0.30
Ile-19	NH (1)	1.0	0.36
Ala-25	NH (1)	0.2	0.27
Ala-25	βH (3)	0.7	0.20
Lys-26	αH (1)	1.0	0.40
Lys-26	βH (2)	1.0	0.43
Lys-26	εH (2)	0.6	0.46
Ala-27	βH (3)	1.0	0.37
Leu-29	γH (1)	0.5	0.22
Leu-29	δ^1H (3)	0.5–1.0	0.39
Leu-29	δ^2H (3)	0.5–1.0	0.25
Arg-42	δH (2)	1.0	0.24
Lys-46	εH (2)	0.6	0.28
Arg-53	αH (1)	0.3	0.12

[a] Number of contributing protons given within parentheses.

[b] Calculated from the nonuniform diffusion model with the parameter values given in the text.

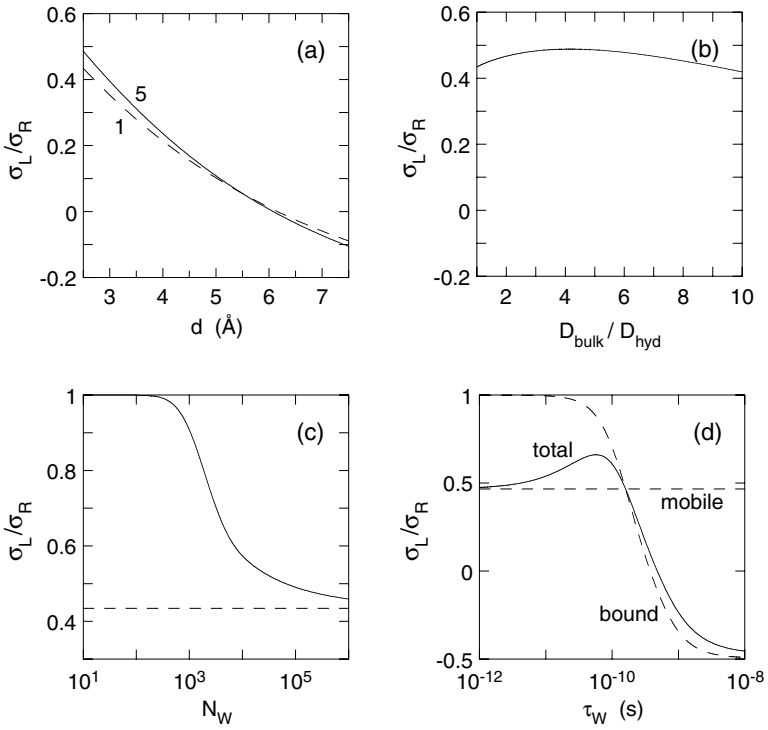

Figure S3. Ratio of water-BPTI cross-relaxation rates in the laboratory (σ_L) and rotating (σ_R) frames at 500 MHz ^{1}H NMR frequency predicted by the nonuniform diffusion model. Unless otherwise noted, the parameter values were taken from Table 2. The subfigures show the dependence of σ_L/σ_R on ***(a)*** the distance of closest approach between water and BPTI protons with the indicated value of D_{bulk}/D_{hyd}, ***(b)*** the ratio of translational mobilities in hydration layer and bulk solvent, ***(c)*** the number of water molecules contributing to the cross-relaxation rates, and ***(d)*** the residence time of a single bound water molecule with the two water protons 3 Å from the BPTI proton. In subfigure (*c*), $D_{hyd} = D_{bulk}$ and the dashed line represents the limit $N_W \rightarrow \infty$. In subfigure (*d*), the dashed curve and line give the σ_L/σ_R ratio produced by the single bound water molecule and all mobile water molecules, respectively.

References

(S1) Otting, G.; Liepinsh, E. *J. Magn. Reson. B* **1995**, *107*, 192–196.

(S2) Sobol, A. G.; Wider, G.; Iwai, H.; Wüthrich, K. *J. Magn. Reson.* **1998**, *130*, 262–271.

(S3) Sklenár, V. *J. Magn. Reson. A* **1995**, *114*, 132–135.

(S4) Driscoll, P. C.; Clore, G. M.; Beress, L.; Gronenborn, A. M. *Biochemistry* **1989**, *28*, 2178–2187.

(S5) Jacobson, A.; Leupin, W.; Liepinsh, E.; Otting, G. *Nucl. Acids Res.* **1996**, *24*, 2911–2918.

(S6) Wood, S. P. et al. *Science* **1986**, *232*, 633–636.

(S7) Otting, G.; Liepinsh, E.; Wüthrich, K. *Science* **1991**, *254*, 974–980.

(S8) Cho, C. H.; Urquidi, J.; Singh, S.; Robinson, G. W. *J. Phys. Chem. B* **1999**, *103*, 1991–1994.

(S9) Noda, K.; Ohashi, M.; Ishida, K. *J. Chem. Eng. Data* **1982**, *27*, 326–328.

(S10) Yergovich, T. W.; Swift, G. W.; Kurata, F. *J. Chem. Eng. Data* **1971**, *16*, 222–226.

(S11) Price, W. S.; Ide, H.; Arata, Y.; Söderman, O. *J. Phys. Chem. B* **2000**, *104*, 5874–5876.

(S12) Kestin, J.; Imaishi, N.; Nott, S. H.; Nieuwoudt, J. C.; Sengers, J. V. *Physica A* **1985**, *134*, 38–58.

(S13) Wlodawer, A.; Walter, J.; Huber, R.; Sjölin, L. *J. Mol. Biol.* **1984**, *180*, 301–329.

(S14) Beeser, S. A.; Goldenberg, D. P.; Oas, T. G. *J. Mol. Biol.* **1997**, *269*, 154–164.

(S15) Gottschalk, M.; Venu, K.; Halle, B. *Biophys. J.* **2003**, *84*, 3941–3958.

(S16) Denisov, V. P.; Peters, J.; Hörlein, H. D.; Halle, B. *Nature Struct. Biol.* **1996**, *3*, 505–509.

(S17) Denisov, V. P.; Halle, B.; Peters, J.; Hörlein, H. D. *Biochemistry* **1995**, *34*, 9046–9051.

(S18) Denisov, V. P.; Halle, B. *J. Mol. Biol.* **1995**, *245*, 698–709.